Extended Greenwood-Williamson Models for Rough Spheres

T. Zhao, Y. T. Feng*
Zienkiewicz Centre for Computational Engineering, Swansea University, UK

Abstract

The current work aims to develop two Extended Greenwood-Williamson (GW) models for spherical particles with surface roughness which can be incorporated into the discrete element modelling (DEM) framework. The defects of the classic GW model when directly adopted in DEM are fully addressed and illustrated by both theoretical and numerical results. The first model, the Extended Elastic GW (E-GW) model, which evaluates the elastic deformation of the asperities and the bulk substrate separately is developed to consider the positive overlap involved in the contact problem. The capability of incorporating the Extended Elastic model into the DEM is illustrated by the comparison between the classic and extended models. The second model, the Extended Elasto-Plastic GW (EP-GW) model, is further developed to consider the plastic deformation of the asperities which reduces the pressure increased by the surface roughness. Numerical comparisons between the E-GW and EP-GW models are also conducted to demonstrate the effect of the plastic deformation on the pressure and deformation distributions in the contact region.

KEYWORDS: Surface roughness; Extended GW model; Elasto-plastic deformation, Normal contact interaction law

1 Introduction

The discrete element method (DEM) is a powerful technology in simulating and predicting the performance of particulate systems. The computational framework of the classic DEM is essentially deterministic, in which the material and geometric properties and the loading conditions are assumed to be known *in prior*. The results obtained from a deterministic analysis are implicitly assumed to represent all the possible scenarios of the system. This is, however, not true for most practical problems where a certain degree of uncertainties is always involved, and therefore traditional deterministic approaches may not be able to treat real problems adequately. A stochastic discrete element modelling methodology which is intended to consider the influence of inherent uncertainties on particulate systems has been developed in our previous work [1, 2].

The geometry variation of the particles is an important random factor in the particulate system. Real granular materials have geometric irregularities at both macroscopic and microscopic levels. However, basic elements commonly used in DEM are regular geometric entities with smooth surface. An increasing attention [3, 4, 5, 6] has been focused on the influence of geometric uncertainty on the mechanical behaviour of the particulate systems while the related work is mostly concentrated on the macroscopic level [7, 8, 9, 10, 11, 12, 13, 14].

*Corresponding author; e-mail: y.feng@swansea.ac.uk

The geometric irregularities at the microscopic level, also called the surface roughness, are more difficult to be accounted for. The surface roughness can be considered by an interaction law which estimates contact forces between particles. This issue is commonly treated by the tangential contact model involving friction. Moreover, the surface roughness will affect the rolling behaviour of particles, and this issue has been considered in the rotational resistance model [15, 16, 17]. However, these methods treat the surface roughness in a deterministic way [18]. Very few attempts have been reported to address the problem of geometric irregularities in randomness. As currently used normal contact laws in DEM, such as the linear and the Hertz contact models, are intended for contact between smooth particles, it may be significant if surface roughness can be included in contact interaction laws in a statistic sense. A first attempt has been made towards this goal in our previous work [1] where a novel random normal interaction law has been proposed, and its application has been demonstrated in [2].

This novel interaction law is based on the classic Greenwood-Williamson (GW) model [19, 21, 20, 22] which is the pioneer work on solving the contact problem between rough surfaces by regarding it as the contact results of a population of asperities. As the theoretical basis of the stochastic approach mentioned, the GW model plays a crucial role in determining the accuracy and rationality of the resulting interaction model. As the early work of treating contact problem between rough spheres, the GW model with ideal assumptions reflects the real contact results less accurately compared to other more recent contact theories [23, 24] while the GW model is chosen as the theories basis because its parameters dependence feature makes it convenient to be incorporated into the discrete element modelling framework. For the contact problem between a smooth sphere and a rough flat surface, the GW model treats the contact between the asperities and the smooth sphere purely elastically and neglects the substrate deformation under the asperities. These theoretical defects lead to some unreasonable results when incorporating the classic GW model into DEM simulations [1].

The classic GW model assumes that the deformation of two interacting rough surfaces can be described by the contacting asperities only. This assumption is valid when the separation between the sphere and the flat surface is large, the asperities are made of the same material as the bulk substrate, and the effects of the deformation of the bulk substrate in the contact problem can be neglected. The contact problem of the material having hard asperities and softer substrate is analysed in [25, 26] which state that the softer bulk deformation may have considerable effects on the surface deformation. An improved contact stiffness model [27] is proposed to resolve this issue in which the asperity and bulk substrate stiffnesses are combined using two springs in series. To our best knowledge, however, no attempt has been reported to solve the contact problem with positive overlap between two rough particles. Therefore, an extended GW model, which can consider a positive overlap between particles by evaluating the deformation of the asperities and the bulk substrate separately, is proposed in the current work for the rough particle contact problem in DEM simulations.

The GW model is better suited for lightly loaded contacts with large separations where the surface asperities deform elastically as the Hertz contact model is adopted for the contact load calculation between the asperity and the sphere. When a positive overlap is involved in the contact, it may be necessary to consider the plastic deformation of the surface asperities. Over the last three decades, several elasto-plastic contact models have been developed for rough surfaces. Based on the concept of volume conservation, Chang *et al.*[28] propose the CEB model in which a critical interference (or overlap) divides the contact regime into elastic and fully plastic components. By recognising the discontinuity involved in the average contact pressure at the critical point of the plastic deformation in the CEB model, Zhao *et al.*[29] present a new elastic-elasto/plastic-fully plastic model (termed the ZMC model) which introduces two critical interferences and bridges the elastic and plastic behaviour of the

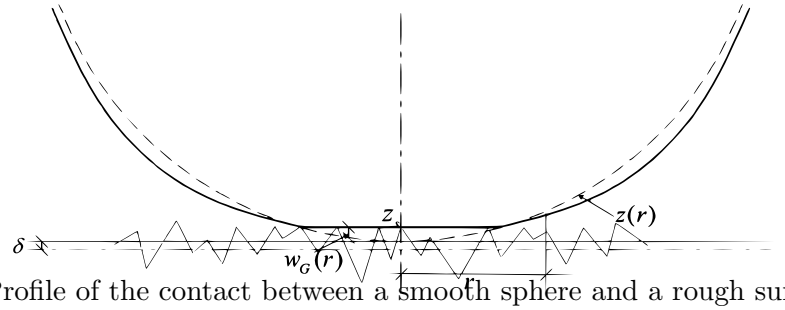

Figure 1: Profile of the contact between a smooth sphere and a rough surface: $\delta \leq 0$

asperity using a cubic polynomial. In addition, based on the work of Kogut and Etsion[30, 31], the finite element analysis has been applied to treat different deformation regimes under which several useful empirical elasto-plastic models have been derived [32, 33]. In addition to the above work that are mainly presented in the tribology literature to treat the plastic deformation involved in contact problem of rough surfaces, there are also a number of elasto-plastic models proposed for contacting (smooth) spheres in DEM [34, 35, 36, 37, 38, 39, 40, 41]. By considering both advantages and disadvantages of these models, an extended elasto-plastic GW model is also developed in the current work to fully take into account the plastic deformation of the asperities.

The paper is organised as follows. The classic GW model is briefly described in the next section and its theoretical inconsistency when involving a positive overlap is identified. The Extended Elastic GW (E-GW) model which can solve the (elastic) contact problem with positive overlap is developed in Section 3 and the comparisons between the classic GW model and the E-GW model are also presented. Following the review of existing elasto-plastic contact models, the E-GW model is further improved in Section 4 leading to the Extended Elasto-Plastic GW (EP-GW) model that can consider the plastic deformation of asperities. The effects of the plastic parameters included in the model are discussed briefly, and the comparison between the E-GW and EP-GW models is also conducted. The conclusion is drawn in Section 5.

2 The classic GW model

In this section, the classic GW model is briefly reviewed first and then a simple extension to general contact cases is described from which a theoretical inconsistency is identified which leads to the development of the extended elastic GW model in the subsequent sections.

2.1 Basic formulation

A rough surface consists of a myriad of asperities or peaks that restrict the real contact area. Due to the complexity of a rough surface, an appropriate mathematical expression is needed to represent a real surface as a profile with asperities that their heights obey a particular statistical distribution, for instance, the Gaussian distribution. This statistical approach to mathematically representing rough surfaces is adopted in the original GW model. By further combining with the Hertz theory, a solution to the contact between rough surfaces is derived. The elaborated explanation of the GW model can be found in the original work [19, 20] or other related work [1, 21, 22].

The contact between two rough spheres can be mathematically transformed into the contact between a deformable smooth sphere and a nominal rigid flat rough surface as shown in

Figure 1. The equivalent radius R and the equivalent standard deviation of the asperity height distribution σ can be obtained by the radii and roughness parameters of the two spheres as

$$\frac{1}{R} = \frac{1}{R_1} + \frac{1}{R_2}; \quad \sigma^2 = \sigma_1^2 + \sigma_2^2 \tag{1}$$

in which subscripts 1 and 2 indicate the sphere number.

Referring to Figure 1(a), δ is the *separation* or *overlap* between the non-deformed configuration of the sphere and the mean line of the flat surface. To make it compatible with the convention of the DEM, δ is assumed to be negative when the two surfaces are in separation, and positive in overlap. The profile of the undeformed sphere (black dashed line) can be described by

$$z(r) = \delta - \frac{r^2}{2R} \tag{2}$$

where r is the distance from the centre to the contact point. Then the separation between the deformed sphere and the nominal flat surface at r is

$$d(r) = w_{_G}(r) - \delta + \frac{r^2}{2R} \tag{3}$$

where $w_{_G}(r)$ is the bulk deformation of the sphere. The overlap of the asperity of height z_s at r with the un-deformed sphere is

$$\delta(r) = z_s - d(r) \tag{4}$$

When $\delta(r) > 0$, the contact force between the sphere and the asperity can be computed by the Hertzian theory

$$f(z_s) = \frac{3}{4} E \beta^{1/2} [z_s - d(r)]^{3/2} \tag{5}$$

in which β is the radius of the top of the asperity and is assumed to be the same for all the asperities; and E is the equivalent Young's modulus of the original two spheres. Further assume that the distribution of the asperity heights obeys the following Gaussian probability density function

$$\phi(z_s) = \frac{1}{\sqrt{2\pi\sigma^2}} \exp\big(-\frac{z_s^2}{2\sigma^2}\big) \tag{6}$$

The probability of having a contact at any given asperity of height z_s is thus

$$\text{prob}(z_s > d(r)) = \int_{d(r)}^{+\infty} \phi(z_s) dz_s \tag{7}$$

Then the contact pressure distribution between the sphere and the asperities over the entire contact area can be expressed as

$$p_{_G}(r) = C \int_{d(r)}^{+\infty} \big[z_s - d(r)\big]^{3/2} \phi(z_s) dz_s \tag{8}$$

with the constant

$$C = \frac{4}{3} E N \beta^{1/2} \tag{9}$$

in which N is the number of summits in the nominal area. The corresponding deformation $w_{_G}(r)$ can be obtained from the solution to the axi-symmetric deformation of an elastic half-space as follows [42]

$$w_{_G}(r) = \frac{4}{\pi E} \int_0^{\bar{a}} \frac{t}{r+t}\, p_{_G}(t)\, \mathbf{K}(k) dt \tag{10}$$

where $\mathbf{K}(k)$ is the complete elliptic integral of first kind with elliptic modulus

$$k = \frac{2\sqrt{rt}}{r+t} \tag{11}$$

and $\bar{a}$ is the radius of the contact area. By integrating the pressure distribution over the contact area, the total contact force $P_{_G}$ between the sphere and the rough surface with overlap δ can be obtained by

$$P_{_G}(\delta, \sigma) = \int_0^{\bar{a}} 2\pi r \, p_{_G}(r) \, dr \tag{12}$$

However, it is numerically challenging to solve the above highly non-linear problem. A set of computational procedures employed to effectively and accurately attain $P_{_G}(\delta, \sigma)$ has been developed in [1].

2.2 A simple extension to positive overlap and theoretical inconsistency

Although the classic GW model has been validated (mainly qualitatively though), extended and applied to many applications, see for instance [20, 28, 42, 43], it is not clear whether the classic GW model is still valid or not for $\delta > 0$, i.e. when there is a positive overlap between the sphere and the nominal flat surface. In this subsection, the simple extension of the GW model without any modification is considered and a theoretical inconsistency will be identified which leads to the proposal of the extended elastic GW model in the next section.

For the convenience of later reference, the corresponding Hertzian solutions for the smooth spheres with $\delta > 0$ are given below:

Contact radius:

$$a_{_H} = \sqrt{R\delta} \tag{13}$$

Pressure distribution $p_{_H}(r)$:

$$p_{_H}(r) = \begin{cases} p_{_{H_0}} \left(1 - \dfrac{r^2}{a_{_H}^2}\right)^{1/2}; \quad p_{_{H_0}} = \dfrac{2E}{\pi} \dfrac{a_{_H}}{R}; & r \le a_{_H} \\ 0; & r > a_{_H} \end{cases} \tag{14}$$

Deformation distribution:

$$w_{_H}(r) = \begin{cases} w_{_{H_0}} \left(1 - \dfrac{r^2}{2a_{_H}^2}\right) = \delta - \dfrac{r^2}{2R}; \quad w_{_{H_0}} = \delta; & r \le a_{_H} \\ \dfrac{a_{_H}^2}{\pi R} \Big[\dfrac{r^2}{a_{_H}^2} - 1 + \left(2 - \dfrac{r^2}{a_{_H}^2}\right) \sin^{-1}\left(\dfrac{a_{_H}}{r}\right) \Big]; & r > a_{_H} \end{cases} \tag{15}$$

Total force:

$$P_{_H}(\delta) = \frac{4}{3} E a_{_H} \delta = \frac{4}{3} E \sqrt{R} \delta^{3/2} \tag{16}$$

Under the simple extension of the GW model, it is theoretically important that the GW model can reduce to the Hertzian solution for smooth spheres when the roughness $\sigma = 0$. However, this is not apparent. In fact, it is easy to verify that directly setting $w_{_G}(r)$ to be the Hertzian deformation $w_{_H}(r)$ in (8) gives rise to a zero pressure distribution $p_{_G}(r) = 0$, which is obviously incorrect when $\delta > 0$.

The issue has been fully explored in [1] which concludes that the classic GW model does recover the Hertzian solution, but as the limit when $\sigma \to 0$ if the parameter μ is assumed to be fixed. The main findings are presented below.

Assuming that when σ is close to zero, both the pressure and deformation distributions of the sphere are close to the Hertzian solutions for the smooth contact case, and can be expressed as

$$p_{_G}(r) = p_{_H}(r) - \Delta p(r); \quad \text{with } \Delta p(r) \ll p_{_H}(r) \tag{17}$$

and

$$w_{_G}(r) = w_{_H}(r) - \Delta w(r); \quad \text{with } \Delta w(r) \ll w_{_H}(r) \tag{18}$$

Note that the minus signs on both the right hand sides of the above two expressions are deliberately assumed and the implication will be highlighted at the end of this subsection.

It is found [1] that $\Delta w(r)$ can be approximately expressed as

$$\Delta w(r) \approx \left[\frac{p_{_H}(r)}{C}\right]^{2/3} = \left(\frac{p_{_{H_0}}}{C}\right)^{2/3}\left(1 - \frac{r^2}{a^2}\right)^{1/3} \tag{19}$$

and the maximum difference between $\Delta w(r)$ and $w_{_H}(r)$ appears at $r = 0$ with

$$\Delta w(0) = \left(\frac{16\sqrt{2}}{3\pi\mu}\frac{\sigma}{\delta}\right)^{2/3} w_0 \tag{20}$$

For a given overlap $\delta > 0$ and a fixed μ, it follows that

$$\lim_{\sigma\to 0} \Delta w(r) = 0 \tag{21}$$

The *linear* relationship between $w(r)$ and $p(r)$ in (10) is also applicable to $\Delta w(r)$ and $\Delta p(r)$:

$$\Delta w(r) = \frac{4}{\pi E}\int_0^{\bar{a}} \frac{t}{r+t}\Delta p(r)\mathbf{K}(k)\, dt \tag{22}$$

It is argued [1] that the following approximation holds

$$\Delta p(r) \approx \Delta p(0) \tag{23}$$

While from (22), it has

$$\Delta p(0) = \frac{E}{2a}\Delta w(0) \tag{24}$$

so

$$\Delta p(r) \approx \frac{E}{2a}\Delta w(0) \tag{25}$$

Thus it is concluded that the classic GW model converges to the Hertzian solution when $\sigma \to 0$:

$$\lim_{\sigma\to 0} w_{_G}(r) = w_{_H}(r); \quad \lim_{\sigma\to 0} p_{_G}(r) = p_{_H}(r) \tag{26}$$

The above theoretical argument is also numerically verified in [1].

Nevertheless, as $p_{_G}$ and $w_{_G}$ are approaching to $p_{_H}$ and $w_{_H}$ but from the negative side (refer to (17) and (18), the following conclusion holds when δ is small

$$P_{_G}(\delta) < P_{_H}(\delta) \tag{27}$$

Clearly this is not physical since the contact force for the two rough spheres cannot be smaller than the smooth case for the same nominal overlap δ, thus revealing that the classic GW model is not theoretically valid for $\delta > 0$, at least for small σ.

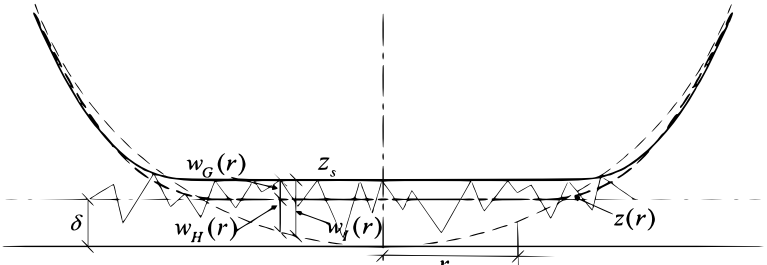

Figure 2: Profile of the contact between a smooth sphere and a rough surface: $\delta \geq 0$

3 The Extended Elastic GW model

The above analysis demonstrates that the GW model cannot handle the condition when $\delta > 0$, which is in accord with the general accepted conclusion that the classic GW model is better suited for light contacts with large separations [28, 33]. This difficulty is due to the assumption made in the GW model that the deformation of the interacting rough surfaces is described by the contacting asperities only, and the bulk deformation under the surface asperities has been ignored. A positive overlap between particles in DEM simulations will definitely make contribution to the contact force. Therefore, the classic GW model cannot be incorporated in the DEM modelling framework without modification.

To take full consideration of the positive overlap, the GW model is extended by evaluating the contributions of both the asperities and the substrate to the deformation. As the asperity deforms elastically in the classic GW model, the resulting extended model is termed the Extended Elastic GW model or the E-GW model.

3.1 Model description

The contact of rough particles in the discrete element modelling can be described by two steps: (a) the contact of the smooth particles with the overlap δ; and (b) an additional displacement due to the surface roughness. Based on this observation, the rough (flat) surface is divided into two parts: the nominal smooth surface and the associated rough asperities, and both parts additively contribute to the deformation of the (smooth) sphere and the final contact force. As shown in Figure 2, the profile in dashed represents the deformed sphere in contact only with the smooth surface (i.e. the Hertizan part); while the profile in solid line represents the final deformed configuration of the sphere in contact with the rough surface. The smooth surface is taken as the datum (the solid central line in Figure 2) which is also the mean height of the asperities.

The contact force due to the smooth part can be obtained from the Hertz law. The pressure distribution $p_{_H}(r)$, the deformation distribution $w_{_H}(r)$ and the total force $P_{_G}(\delta)$ are given by (14), (15) and (16) respectively.

The additional contact force caused by the asperities is determined by the classic GW model. The profile in dashed green line can be regarded as the undeformed sphere without considering the effect of the asperities which is described by

$$z(r) = w_{_H}(r) + \frac{r^2}{2R} - \delta \tag{28}$$

Then the separation between the deformed sphere after contacting with asperities and the deformed sphere after contacting with the smooth surface is

$$d(r) = w_{_G}(r) + z(r) \tag{29}$$

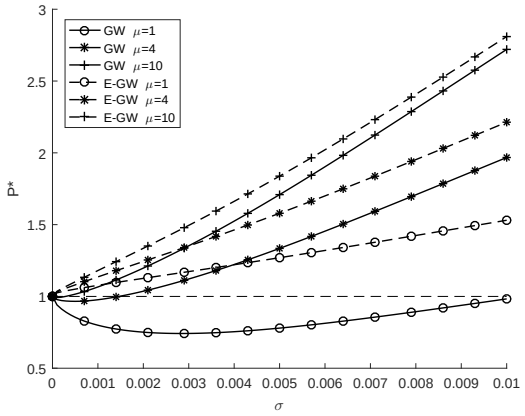

Figure 3: Comparison of non-dimensional total contact forces between the GW and E-GW models for different degrees of roughness

The overlap between the asperity and the dashed green line is

$$\delta_{G}(r) = z_s - w_{G}(r) - z(r) \tag{30}$$

Then the contact pressure distribution $p_{G}(r)$ and deformation distribution $w_{G}(r)$ can be expressed as

$$p_{G}(r) = C \int_{d(r)}^{+\infty} \left[\delta_{G}(r)\right]^{3/2} \phi(z_s) dz_s \tag{31}$$

$$w_{G}(r) = \frac{4}{\pi E} \int_{0}^{\bar{a}} \frac{t}{r+t}\, p_{G}(t)\, \mathbf{K}(k) dt \tag{32}$$

The contact pressure is the sum of the Hertz pressure and the GW pressure. Thus the total pressure distribution $p(r)$ and deformation distribution $w(r)$ of the sphere can be expressed by

$$p(r) = p_{H}(r) + p_{G}(r) \tag{33}$$

$$w(r) = w_{H}(r) + w_{G}(r) \tag{34}$$

The total contact force $P(\delta, \sigma)$ is the summation of the Hertz force $P_{H}(\delta)$ and the rough GW contribution $P_{G}(\delta, \sigma)$ defined by (12) as

$$P(\delta, \sigma) = P_{H}(\delta) + P_{G}(\delta, \sigma) \tag{35}$$

By utilising the fact that the Hertz contribution is zero when δ is negative, the above extended GW model includes the classic case as a special case. For the rough part, p_{G} can be set to be zero when $\delta < -3\sigma$ because the probability that a summit z_s lies in the range $[-3\sigma, +3\sigma]$ is 99.9%.

3.2 Comparison between the classic and the extended models

The classic GW model and the E-GW model are compared in this subsection. Unlike in the traditional tribology where the interest is mainly focused on the evolution of the separation and effective contact area under a varied normal load, the attention in the current work is concentrated on the change of the total contact force with an increasing surface roughness under the same overlap between particles. Therefore, the non-dimensional total contact

force, the pressure distribution and the deformation distribution under the same overlap are compared between the two models.

Figure 3 shows the relationship between the surface roughness σ and the non-dimensional total contact force $P^*(= P/P_H)$ with a positive overlap $\delta = 0.01$. The roughness σ increases from 0 to 0.01 and three different values, 1, 4 and 10, are chosen for the non-dimensional parameter μ. The rough surface is supposed to result in a larger normal contact force than the smooth surface with the same overlap, which means the non-dimension total contact force P^* should always be greater than 1 and should also increase with the increase of the degree of roughness σ.

However, it is evident from Figure 3 that when σ is approaching to zero, the non-dimensional contact forces P^* obtained from the GW model are smaller than 1, meaning the contact forces of rough particles are smaller than those of smooth particles. This is physically incorrect and is consistent with the theoretical predication presented in Section 2.2. On the other hand, the extended model correctly captures the phenomenon that rougher surfaces produce larger contact forces than smoother surfaces under the same overlap.

The pressure and deformation distributions based on the classic GW model and the E-GW model are also compared and shown in Figure 4(a) and Figure 5(a) respectively. To make the comparison more apparent, the differences of these distributions with the corresponding Hertz solutions are depicted in Figure 4(b) and Figure 5(b). The results are obtained with the same positive overlap $\delta = 0.01$, the same non-dimensional parameter $\mu = 4$ and three different surface roughness levels $\sigma = 10^{-5}, 10^{-4}$, and 10^{-3}.

The fact that the pressure and the deformation gradually approach to the Hertz solution as σ decreases when the surface becomes smoother can be seen for both models but in different fashions. The classic GW model achieves this from below the Hertz solution in most of the contact region which is again conforming to the theoretical analysis in Section 2.2. Also the surface asperities reduce the pressure and deformation in the original contact area between the sphere and the smooth surface but lead to a significantly larger effective contact area. On the contrary, the E-GW model approaches to the Hertz solution from above which reflects the fact that, as the surface becomes rougher, both pressure and deformation increase inside and outside the original contact area. The increase of pressure and deformation in the original Hertz contact area is almost same because the sphere has conforming contact with the smooth flat. There is a decreasing trend of the difference outside the original Hertz contact area because the curved profile of the sphere again affects the overlap.

In DEM simulations, a positive overlap is defined between two smooth particles (for dry mechanical contact only), the asperities added on the smooth surface should cause additional pressure and deformation. Therefore, it can be concluded that the current extended model is more realistic for the contact situation with a positive overlap.

4 The Extended Elasto-Plastic GW model

When a positive overlap exists between two rough particles, the asperities may undergo substantial deformation. Therefore, the major assumption made in the classic GW model that the asperity deforms elastically may no longer hold in this case. It is thus necessary to consider the plastic deformation of asperities in the extended model.

As mentioned in Section 1, a number of plastic contact models have been developed both for the contact problem of rough surfaces and for the single contact between two smooth

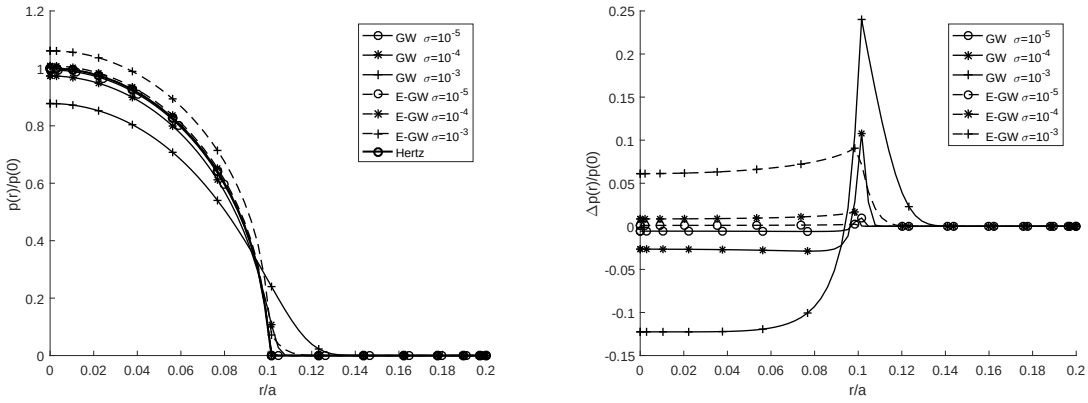

(a) Pressure distribution (b) Pressure difference distribution

Figure 4: Comparison of pressure distributions over the contact zone

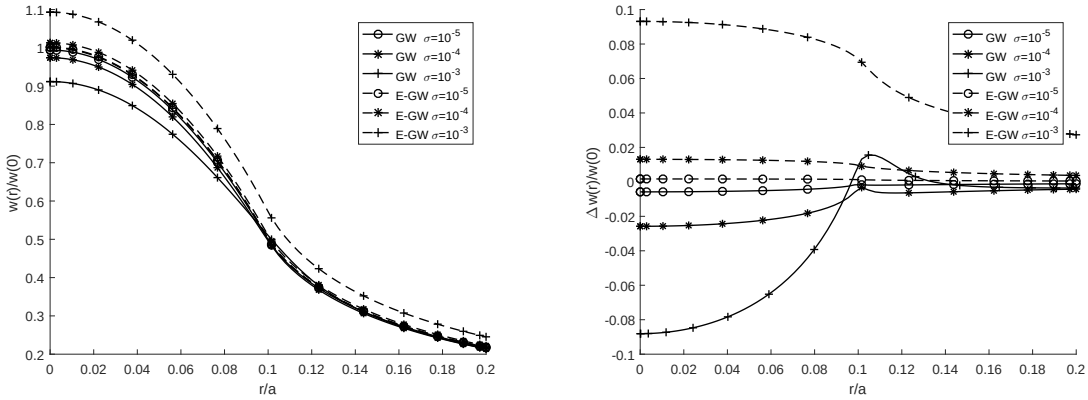

(a) Deformation distribution (b) Deformation difference distribution

Figure 5: Comparison of deformation distributions with over the contact zone

spheres. These plastic contact models can be classified into two categories: *analytical* [28, 29, 36, 37] and *semi-analytical* [30, 31, 32, 33]. Both categories have their own advantages and disadvantages.

The analytical contact models are based on the general physical reality that materials can exhibit different deformation behaviours during the contacting process which can be summarised into different regimes. The earlier work only contains two regimes: elastic and plastic. While the three regimes model (elastic, elasto-plastic, and fully plastic) are now more accepted. The critical overlap is proposed to indicate the inception of each regime which can be defined by the material properties. For the elastic regime, the force-displacement relationship is based on the Hertz model obeying a power law with the exponent of 1.5. For the plastic regime, a linear law is used for the force-displacement relationship. For the transition regime from elastic to plastic, the power law for the elastic regime and the linear law for the plastic regime are joined by some mathematical methods. The analytical models can be readily applied to simulate different materials while the simple assumptions used in these models make it almost impossible to fit experiments perfectly.

The semi-analytical models are based on experiments or numerical simulations which can predict the deformation behaviour of specific materials and geometries [44, 45], but the parameters need to be re-calibrated by either time-consuming experiments or numerical calculations

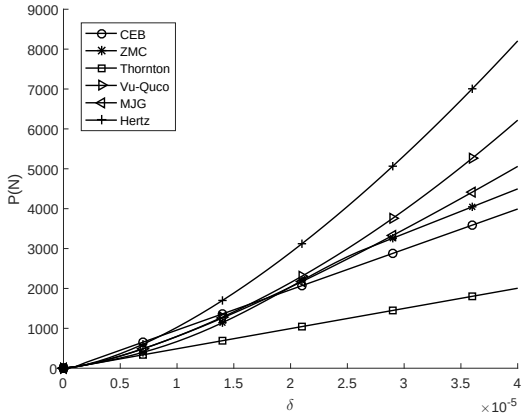

Figure 6: Force displacement relationships based on different contact models

for each material to be simulated.

To observe the deformation behaviour described by different elasto-plastic models, the force displacement relationships for six contact models, denoted as CEB[28], ZMC[29], Thornton[36], Vu-Quoc[38], MJG[46] and Hertz respectively, are depicted in Figure 6 for illustrative purpose. The material and geometric parameters used to generate the curves are taken from [38], and listed in Table 1. Note that the Vu-Quoc model is only valid for the specific material and geometry.

Table 1: Parameters used in the contact models

Variable	Radius (m)	Young's modulus (GPa)	Poisson's ratio	Hardness coefficient	Yield stress (MPa)	Yield force coefficient
	R	E	ν	K	σ_y	A_Y
Value	0.1	76.923	0.3	0.6	100	1.61

The CEB, ZMC and Thornton models are analytical contact models, while the Vu-Quoc and MJG models are semi-analytical. The CEB and Thornton models contain two deformation regimes: elastic and plastic. As shown in Figure 6, the Thornton model predicts a much smaller contact force than the other four elasto-plastic contact models. In the CEB model, the force is even larger than that obtained from the Hertz model at the initial part of the plastic regime. Compared to the CEB and Thornton models, the ZMC model with three deformation regimes is closer to the semi-analytical models (Vu-Quoc and MJG).

To introduce an elasto-plastic contact model for the contact between rough surfaces, the integral domain of the pressure distribution (Equation 8) needs to be divided into different regions according to different critical overlaps. The contact forces between the asperities and the sphere are evaluated by the corresponding force-displacement laws. No elasto-plastic contact model is, however, widely accepted as the best choice at the moment. Considering both generality and simplicity of the formulas, an analytical elasto-plastic model is desired to be applied into our extended GW model. The resulting contact model is termed as the Extended Elasto-plastic GW (EP-GW) model. In the current work, the ZMC model [29] is adopted as it can predict the deformation behaviour more accurately compared to other analytical models.

In the ZMC model, the three deformation regimes are determined by two critical overlaps, δ_{ep} and δ_p. The first *elasto-plastic* critical overlap δ_{ep} is defined at the point when the mean contact pressure p_a reaches KH and elasto-plastic deformation occurs, which yields

$$\delta_{ep} = \left(\frac{3\pi KH}{4E}\right)^2 \beta \tag{36}$$

where H and K are respectively the hardness and hardness coefficient of the material concerned. The second *plastic* critical overlap δ_p is defined at the point when the mean contact pressure p_a reaches H at which fully plastic deformation occurs. There is no theoretical solution available for δ_p, however. Based on experimental results and a simple analysis, the following relation is suggested in [29]

$$\delta_p \geq 54\,\delta_{ep} \tag{37}$$

When $\delta < \delta_{ep}$, the asperity deforms elastically. The mean contact pressure p_{a_e} and the contact area A_e are obtained from the Hertz theory

$$p_{a\_e} = \frac{4E}{3\pi}\sqrt{\frac{\delta}{\beta}}; \quad A_e = \pi\beta\delta \tag{38}$$

When $\delta > \delta_p$, the asperity deforms fully plastically. The mean contact pressure remains constant at H. The contact area, according to Abbott and Firestone [47], is equal to the geometrical intersection of the flat surface with the original undeformed profile of the asperity. Thus

$$p_{a\_p} = H; \quad A_p = 2\pi\beta\delta \tag{39}$$

When $\delta_{ep} < \delta < \delta_p$, the asperity deforms elasto-plastically. The mean contact pressure p_{a_ep} and the contact area A_{ep} as functions of the overlap δ become complex. The relation between p_{a_ep} and δ is derived based on the results from Francis [48] which can be characterised by a logarithmic function. Further considering the continuity of the mean pressure at the point of $\delta = \delta_{ep}(p_a = KH)$ and $\delta = \delta_p(p_a = H)$, the mean contact pressure in the elasto-plastic regime is given by

$$p_{a\_ep} = H\left[1 - (1-K)\frac{\ln(\delta_p/\delta)}{\ln(\delta_p/\delta_{ep})}\right] \tag{40}$$

The relation between the contact area A_{ep} and the overlap δ is derived by joining the expressions for $A_e = \pi\beta w$ and $A_p = 2\pi\beta w$ smoothly using a cubic polynomial formula.

$$A_{ep} = \pi\beta\delta\left[1 + 3\lambda_{ep}^2(\delta) - 2\lambda_{ep}^3(\delta)\right] \tag{41}$$

where

$$\lambda_{ep}(\delta) = \frac{\delta - \delta_{ep}}{\delta_p - \delta_{ep}}; \quad \lambda_{ep}(\delta_{ep}) = 0; \quad \lambda_{ep}(\delta_p) = 1$$

Hence, the contact force of an asperity and the smooth sphere can be expressed as a function of the overlap δ by

$$f(\delta) = p_a A = \begin{cases} \dfrac{4}{3}E\beta^{1/2}\delta^{3/2}; & \delta \leq \delta_{ep} \\ \pi H\beta[1-(1-K)D_1(\delta)]D_2(\delta); & \delta_{ep} < \delta \leq \delta_p \\ 2\pi H\beta\delta; & \delta > \delta_p \end{cases} \tag{42}$$

where

$$\begin{aligned} D_1(\delta) &= \frac{\ln(\delta_p/\delta)}{\ln(\delta_p/\delta_{ep})} \\ D_2(\delta) &= \left[1 + 3\lambda_{ep}^2(\delta) - 2\lambda_{ep}^3(\delta)\right]\delta \end{aligned} \tag{43}$$

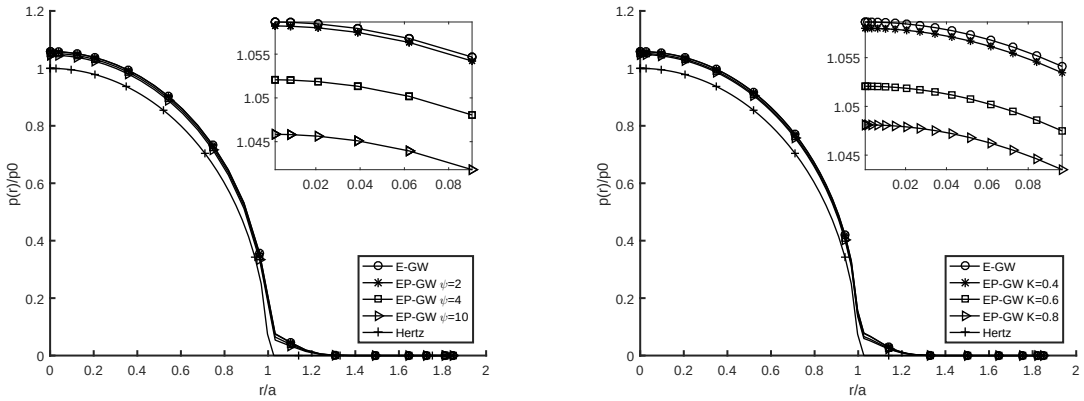

(a) $K = 0.6$ (b) $\psi = 4$

Figure 7: Comparisons of the pressure distribution between different contact models

Then, similar to to (8), the pressure distribution $p_{_G}(r)$ after considering the whole rough surface can be expressed as

$$p_{_G}(r) = N \int_{d(r)}^{+\infty} f(z_s - d(r))\phi(z_s)dz_s \tag{44}$$

Or more explicitly

$$\begin{aligned} p_{_G}(r) = & C \int_{d(r)}^{d(r)+\delta_{ep}} \left[\delta_{_G}(r)\right]^{3/2} \phi(z_s)dz_s \\ & + \frac{3C\sigma^{1/2}}{2K\psi} \left\{ \int_{d(r)+\delta_{ep}}^{d(r)+\delta_p} \left[1-(1-K)D_1(\delta_{_G}(r))\right] D_2(\delta_{_G}(r))\phi(z_s)dz_s \right. \\ & \left. + \int_{d(r)+\delta_p}^{+\infty} \delta_{_G}(r)\phi(z_s)dz_s \right\} \end{aligned} \tag{45}$$

where ψ is the plastic index defined by Greenwood and Williamson[19] as

$$\psi = (\delta_{ep}/\sigma)^{-1/2} \tag{46}$$

The critical overlap δ_{ep} can be expressed as

$$\delta_{ep} = \frac{\sigma}{\psi^2} \tag{47}$$

Now this EP-GW model can consider the plastic deformation of the asperities by introducing two more parameters, the plastic index ψ and the hardness coefficient K, compared to the E-GW model. The EP-GW model recovers the E-GW model when $\psi = 0$ as $\delta_{ep} = \infty$.

The Hertz, E-GW and EP-GW models are compared below. The effects of the roughness parameters σ and μ on the contact features have been discussed in our previous work[1]. Only the effects of the plastic parameters ψ and K are investigated here. The other parameters are fixed and have the same values for all the models: $\delta = 0.01, \sigma = 0.001, \mu = 4$.

Figure 7(a) illustrates the pressure distribution for three different values of $\psi = 2, 4$ and 10 but the same value of $K = 0.6$. As can be seen, the pressure calculated from the E-GW model (blue line) has the largest value as expected, which reflects the elastic effects of the surface roughness. The increase of the plastic index reduces the pressure increased by the

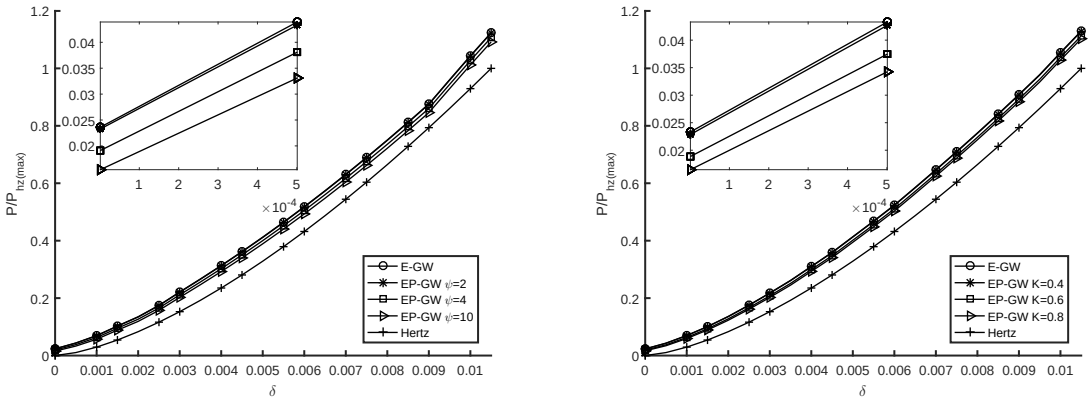

(a) $K = 0.6$ (b) $\psi = 4$

Figure 8: Comparisons of the force-displacement relationship between different contact models

surface roughness as more asperities deform plastically. Figure 7(b) illustrates the pressure distribution for three different values of $K = 0.4, 0.6$ and 0.8 but a fixed value of $\psi = 4$. Similar results can be observed that the increase of K reduces the pressure increased by the surface roughness.

The force-displacement relationship is the most interested issue when a rough surface contact model is applied to the DEM simulation. The relationships based on different models for a particularly given set of parameter values are illustrated in Figure 8. As expected, the increase of both ψ and K reduces the normal load increased by the surface roughness. Note, however, that the underlay smooth particle contact is still assumed linearly elastic.

It can be observed from Figure 7 and Figure 8 that the effects of the plastic deformation are not significant compared to the difference induced by the surface roughness between the Hertz model and the E-GW model. It can be explained in two ways, when δ is small almost all the asperities deform in the elastic region while when δ is large the deformation of the substrate accounts for the main part compared to which the plastic deformation of the asperities is not obvious.

5 Conclusion

The basic defects of the classic GW model when incorporated into the DEM have been fully addressed in the current work by both theoretical analysis and numerical simulations. The Extended Elastic GW model has been developed to consider a positive overlap by evaluating the deformation of the asperity and the substrate separately. The applicability of the Extended Elastic GW model is illustrated by the comparison with the classic GW model. By further considering the plastic deformation of the asperities using the ZMC elasto-plastic model, the Extended Elasto-Plastic GW model has been established. The numerical results show that the plastic deformation of the asperities reduce the pressure increased by the surface roughness. Both extended GW models can now be applied to DEM simulations. It is highlighted, however, that due to complex physical phenomena involved, significant assumptions made, and some mathematical approximation adopted, the two extended models may need to be appropriately validated, which is beyond the scope of the current work.

References

[1] Feng, Y.T., Zhao, T., Kato, J. and Zhou, W. Towards stochastic discrete element modelling of spherical particles with surface roughness: A normal interaction law. *Computer Methods in Applied Mechanics and Engineering.* 315: 247-272, 2017.

[2] Zhao, T., Feng, Y.T., and Wang, M. An extended Greenwood-Williamson model based normal interaction law for discrete element modelling of spherical particles with surface roughness. *International Journal for Numerical and Analytical Methods in Geomechanics.* 2018 (in press).

[3] Cho, N.A., Martin, C.D. and Sego, D.C. A clumped particle model for rock. *International Journal of Rock Mechanics and Mining Sciences.* 44(7): 997-1010, 2007.

[4] Hryciw, R.D., Zheng, J. and Shetler, K. Particle roundness and sphericity from images of assemblies by chart estimates and computer methods. *Journal of Geotechnical and Geoenvironmental Engineering.* 142(9): 04016038, 2016.

[5] Jensen, R.P., Bosscher, P.J., Plesha, M.E. and Edil, T.B. DEM simulation of granular mediastructure interface: effects of surface roughness and particle shape *International Journal for Numerical and Analytical Methods in Geomechanics.* 23(6):531-547, 1999.

[6] Wang, L., Park, J.Y. and Fu, Y. Representation of real particles for DEM simulation using X-ray tomography. *Construction and Building Materials.* 21(2): 338-346, 2007

[7] Lu, M. and McDowell, G.R. The importance of modelling ballast particle shape in the discrete element method. *Granular matter.* 9(1-2): 69, 2007

[8] Ferellec, J.F. and McDowell, G.R. A simple method to create complex particle shapes for DEM. *Geomechanics and Geoengineering: An International Journal.* 3(3): 211-216, 2008

[9] Shamsi, M.M. and Mirghasemi, A.A. Numerical simulation of 3D semi-real-shaped granular particle assembly. *Powder technology.* 28(2): 431-446, 2012

[10] Zhou, W., Ma, G., Chang, X.L. and Duan, Y. Discrete modeling of rockfill materials considering the irregular shaped particles and their crushability. *Engineering Computations.* 32(4):1104-1120, 2015.

[11] Feng, Y.T., and Owen, D. R. J. A 2D polygon/polygon contact model: algorithmic aspects. *Engineering Computations.* 21: 265-277, 2004

[12] Han, K., Feng, Y.T., and Owen, D. R. J. Polygon-based contact resolution for superquadrics. *International Journal for Numerical Methods in Engineering.* 66: 485501.2006

[13] Feng, Y.T., Han, K., and Owen, D. R. J. Energy-conserving contact interaction models for arbitrarily shaped discrete elements. *Computer Methods in Applied Mechanics and Engineering.* 205-208: 169-177, 2012

[14] Feng, Y.T., Han, K., and Owen, D. R. J. A generic contact detection framework for cylindrical particles in discrete element modelling. *Computer Methods in Applied Mechanics and Engineering.* 315: 632-651, 2017

[15] Iwashita, K. and Oda, M. Rolling resistance at contacts in simulation of shear band development by DEM. *Journal of engineering mechanics.* 124(3): 285-292, 1998

[16] Jiang, M.J., Yu, H.S. and Harris, D. A novel discrete model for granular material incorporating rolling resistance. *Computers and Geotechnics.* 32(5): 340-357, 2005

[17] Huang, X., Hanley, K.J., O'Sullivan, C. and Kwok, C.Y. Implementation of rotational resistance models: a critical appraisal. *Particuology.* 34: 14-23, 2017

[18] Wilson, R., Dini, D. and Van Wachem, B. The influence of surface roughness and adhesion on particle rolling. *Powder Technology.* 312: 321-333, 2017

[19] Greenwood, J.A. and Williamson, J.P. Contact of nominally flat surfaces. *Proceedings of the Royal Society of London A: Mathematical, Physical and Engineering Sciences.* 295(1442): 300-319, 1966

[20] Greenwood, J.A. and Tripp, J.H. The elastic contact of rough spheres. *Journal of Applied Mechanics.* 34(1): 153-159, 1967

[21] Beheshti, A. and Khonsari, M.M. On the contact of curved rough surfaces: contact behavior and predictive formulas. *Journal of Applied Mechanics.* 81(11): 111004, 2014

[22] Beheshti, A. and Khonsari, M.M. Asperity micro-contact models as applied to the deformation of rough line contact. *Tribology International.* 52: 61-74, 2012

[23] Pastewka, L. and Robbins, M.O. Contact area of rough spheres: Large scale simulations and simple scaling laws. *Applied Physics Letters.* 108(22): 221601, 2016

[24] Pohrt, R. and Popov, V.L. Contact mechanics of rough spheres: Crossover from fractal to hertzian behavior. *Advances in Tribology.* 2013: 1-4, 2013

[25] Iida, K. and Ono, K. Design consideration of contact/near-contact sliders based on a rough surface contact model. *Journal of tribology.* 125(3):562-570, 2003

[26] Shi, X. and Polycarpou, A.A. Investigation of contact stiffness and contact damping for magnetic storage head-disk interfaces. *Journal of tribology.* 130(2):021901, 2008

[27] Yeo, C.D., Katta, R.R. and Polycarpou, A.A. Improved elastic contact model accounting for asperity and bulk substrate deformation. *Tribology letters* 35(3):191-203, 2009

[28] Chang, WR., Etsion, I. and Bogy, D BASME An elastic-plastic model for the contact of rough surfaces. *Journal of tribology.* 109: 257-263, 1987

[29] Zhao, Y., Maietta, D.M. and Chang, L. An asperity microcontact model incorporating the transition from elastic deformation to fully plastic flow. *Journal of Tribology.* 122(1): 86-93, 2000

[30] Kogut, L. and Etsion, I. Elastic-plastic contact analysis of a sphere and a rigid flat. *Journal of applied Mechanics.* 69(5): 657-662, 2002

[31] Kogut, L. and Etsion, I. A finite element based elastic-plastic model for the contact of rough surfaces. *Tribology transactions.* 46(3):383-390, 2003

[32] Jackson, R.L. and Green, I., 2005. A finite element study of elasto-plastic hemispherical contact against a rigid flat. *Journal of tribology.* 127(2):343-354, 2005

[33] Jackson, R.L. and Kogut, L. A comparison of flattening and indentation approaches for contact mechanics modeling of single asperity contacts. *Journal of Tribology.* 128(1):209-212, 2006

[34] Walton, O.R. and Braun, R.L. Viscosity, granulartemperature, and stress calculations for shearing assemblies of inelastic, frictional disks. *Journal of rheology.* 30(5):949-980, 1986

[35] Walton, O.R. Numerical simulation of inelastic, frictional particle-particle interactions. *Particle two phase flow.* 25, 1993

[36] Ning, Z. and Thornton. Elastic-plastic impact of fine particles with a surface. *Powders and grains.* 93:33-38, 1993

[37] Thornton, C. Coefficient of restitution for collinear collisions of elastic-perfectly plastic spheres. *Journal of Applied Mechanics.* 64(2):383-386, 1997

[38] Vu-Quoc, L. and Zhang, X. An elastoplastic contact forcedisplacement model in the normal direction: displacementdriven version. *In Proceedings of the Royal Society of London A: Mathematical, Physical and Engineering Sciences.* 455(1991):4013-4044, 1999

[39] Vu-Quoc, L., Zhang, X. and Lesburg, L. A normal force-displacement model for contacting spheres accounting for plastic deformation: force-driven formulation. *Journal of Applied Mechanics.* 67(2):363-371, 2000

[40] Vu-Quoc, L., Zhang, X. and Lesburg, L. Normal and tangential force-displacement relations for frictional elasto-plastic contact of spheres. *International journal of solids and structures.* 38(36-37):6455-6489, 2001

[41] Rathbone, D., Marigo, M., Dini, D. and van Wachem, B. An accurate force-displacement law for the modelling of elastic-plastic contacts in discrete element simulations. *Powder Technology.* 282:2-9, 2015

[42] Johnson, K.L. Contact Mechanics, Cambridge University Press, Cambridge, 1985.

[43] Jackson, R.L. and Green, I. A statistical model of elasto-plastic asperity contact between rough surfaces. *Tribology International.* 39: 906-914, 2006

[44] Ma, D. and Liu, C. Contact law and coefficient of restitution in elasto-plastic spheres. *Journal of Applied Mechanics* 82(12):121006, 2015

[45] Wang, H., Yin, X., Qi, X., Deng, Q., Yu, B. and Hao, Q. Experimental and theoretical analysis of the elastic-plastic normal repeated impacts of a sphere on a beam. *International Journal of Solids and Structures* 109:131-142, 2017

[46] Ghaednia, H., Pope, S.A., Jackson, R.L. and Marghitu, D.B. A comprehensive study of the elasto-plastic contact of a sphere and a flat. *Tribology International* 93:78-90, 2016

[47] Abbott, E.J. and Firestone, F.A. Specifying surface quality: a method based on accurate measurement and comparison. *SPIE MILESTONE SERIES MS.* 107: 63-63, 1995

[48] Francis, H.A. Phenomenological analysis of plastic spherical indentation. *Journal of Engineering Materials and technology.* 98(3): 272-281, 1976